Research Square

Preprints are preliminary reports that have not undergone peer review.
They should not be considered conclusive, used to inform clinical practice,
or referenced by the media as validated information.

Ulvan from Ulva ohnoi macroalgae : Green extraction method and physicochemical characterization of the ulvan

Kessi Crescencio
Universidade de Sorocaba
Venâncio Amaral
Universidade de Sorocaba
Alexandro Souza
State University of Campinas
Cecilia Barros
Universidade de Sorocaba
Juliana Souza
Universidade de Sorocaba
Denicezar Baldo
Universidade de Sorocaba
José Oliveira
Universidade de Sorocaba
Paulo Horta
Universidade Federal de Santa Catarina
Eduardo Bastos
Universidade Federal de Santa Catarina
Ronan Behling
Fernando Batain
Universidade de Sorocaba
Patricia Severino
Universidade Tiradentes
Thais Almeida
Universidade de Sorocaba
Eliana Souto
University of Porto
Marco Chaud
chaudmarco@gmail.com

Universidade de Sorocaba

Article

Keywords: Ulva ohnoi, ulvan, green macroalgae, sulfated hetero-polysaccharide, green extract methods

Posted Date: August 20th, 2024

DOI: https://doi.org/10.21203/rs.3.rs-4751748/v1

License: This work is licensed under a Creative Commons Attribution 4.0 International License.
Read Full License

Additional Declarations: No competing interests reported.

Ulvan from *Ulva ohnoi* macroalgae: Green extraction method and physicochemical characterization of the ulvan

Kessi Crescencio[1], Venâncio Amaral[1], Alexandro Souza[2], Cecilia Barros[1], Juliana Souza[1], Denicezar Baldo[3], José Oliveira[3], Paulo Horta[4], Eduardo Bastos[4], Ronan Behling[5], Fernando Batain[8], Patricia Severino[6], Thais Almeida[1], Eliana Souto[7]*, Marco Chaud[1]*

1. Laboratory of Biomaterials and Nanotechnology of UNISO (LaBNUS), University of Sorocaba, Sorocaba, 18023-000, São Paulo, Brazil
2. Department of Materials and Bioprocesses Engineering, School of Chemical Engineering, University of Campinas, Campinas, São Paulo, Brazil
3. Applied Nuclear Physics Laboratory of UNISO (LAFINAU), University of Sorocaba, Sorocaba, 18023-000, São Paulo, Brazil
4. Phycology Laboratory (LAFIC), Federal University of Santa Catarina, Florianopolis, Santa Catarina, Brazil
5. Anton Paar Brazil, Vila Clementino, São Paulo, São Paulo, Brazil
6. Institute of Technology and Research, Tiradentes University, Murilo Dantas, Aracaju, Sergipe, Brazil
7. Laboratory of Pharmaceutical Technology, Faculty of Pharmacy, University of Porto, 4050-313 Porto, Portugal
8. College of Pharmacy, University of Sorocaba, 18023-000 Sorocaba, São Paulo, Brazil

Correspondent authors: Eliana B Souto (souto.eliana@gmail.com);
Marco Vinícius Chaud (marco.chaud@prof.uniso.br; chaudmarco@gmail.com)

Abstract

Ulvan belongs to the class of sulfated heteropolysaccharide and is the main component of the seaweed *Ulva ohnoi* (*U. ohnoi*). Ulvan has a chemical structure similar to fucoidan, chondroitin sulfate, and hyaluronic acid, which are commonly used to develop drug delivery systems. Due to the potential biomedical applications of sulfated and non-sulfated polysaccharides, this work aimed to develop an environmentally friendly method for extracting ulvan from U. ohnoi with high yield and purity. A novel method for the extraction of ulvan is proposed and demonstrated successfully. Various characterization techniques were employed to evaluate the presence of sulfated ions, proteins, elements trace, and crystallinity. The structure, morphology, and physical-chemical properties of ulvan were characterized by electron microscopy (SEM), scanning transmission electron microscopy (TEM), X-ray diffraction (DRX), Infra-red spectrometry (FTIR), DSC-calorimetry and hydrogen-1 nuclear magnetic resonance (^{1}HNMR). Analysis of the results revealed a fibrous, semi-crystalline structure with regular pores, a yield greater than 25%, and a degree of purity greater than 94%. A search for chemical compounds revealed low protein content, high sulfur content, presence of mineral salts, and total absence of heavy metals. Besides, the results demonstrate that the methodology employed allowed to obtain ulvan with a high degree of purity.

Keywords: *Ulva ohnoi*; ulvan; green macroalgae; sulfated hetero-polysaccharide; green extract methods.

Introduction

Ulvales (Chlorophyta) comprises green marine algae distributed along the coast of all terrestrial oceans and in freshwater reservoirs. Among the species that make up this order of algae and *Ulva* genus, the *U. fasciata, U. rigida, U. pertusa, U. lactuca* and *U. ohnoi* are those that attract the most attention and have been used as a source of pharmaceuticals nutraceuticals [1, 2], (bio)fertilizers [3] and for polluted water treatment [4]. However, due to their high proliferation capacity and the possibility of accumulating heavy metals, even under unfavorable environmental conditions, these invasive algae have been associated with harmful to the aquatic environment and to the populations that live on the banks of rivers and lakes and the sea coast [5–7].

The species *U. ohnoi* was first identified by Hiraoka et al. [8] based on DNA sequencing and comparison with the other species of green algae of the genus *Ulva*. *U. ohnoi* is easily adapted for cultivation in a controlled environment and is a relevant source of biomass, polysaccharides, and proteins [8, 9]. Bastos et al. [6] first identified this species of green seaweed in Brazil's Fernando de Noronha archipelago on the country's northeast coast [6, 10]

Studies have been carried out to increase the commercial value of green algae, particularly about ulvan and other sulfated heteropolysaccharides, which represent a unique compound of the anionic sulfated heteropolysaccharides soluble in water. The chemical structure of this heteropolysaccharide features glucuronic acid, iduronic acid, rhamnose, xylose, and sulfate groups. These polymeric chain are mainly compose of repeated disaccharide units of the type β-D-glucuronic acid (1→4)-α-L-rhamnose-3-sulfate and α-L-iduronic acid (1→4)-α-L-rhamnose-3-sulfate [11–13].

Ulvan has unique chemical structural properties, and it shares similarities with glycosaminoglycans such as hyaluronic acid and chondroitin sulfate. However, despite ulvan sharing glucuronic acid in common with all glycosaminoglycans and the sulfate group with chondroitin sulfate, ulvan's chemical structure lacks the amide group found in the hyaluronic acid and chondroitin sulfate chain [14, 15]. The similarities and differences between the chemical structure of ulvan and the chemical structures of hyaluronic acid and chondroitin sulfate are shown in **Figure 1**. Hyaluronic acid and chondroitin sulfate are important heteropolysaccharides used to maintain homeostasis and the biomechanical integrity of tissues. Additionally, they also promote healing at the cellular level and fluids and perform essential physiological, structural, and lubricating functions [16–18]. Ulvan, unlike polysaccharides from non-algal sources, has more sulfate groups in its structure. The sulfate groups contribute

more significant biological activities than their counterpart non-sulfated polysaccharides, which show antiviral, anticoagulant, antioxidant, anticancer, antitumor, and anti-inflammatory properties [19–21]. The non-adhesive property of native sulfated polysaccharides prevents microorganisms' adhesion to surfaces, and it has shown promise in inhibiting the formation of biofilms [22]. These effects and intrinsic and unique properties attributed to the ulvan have increased researchers' interest in its potential application in medicine and biomedical engineering [23].

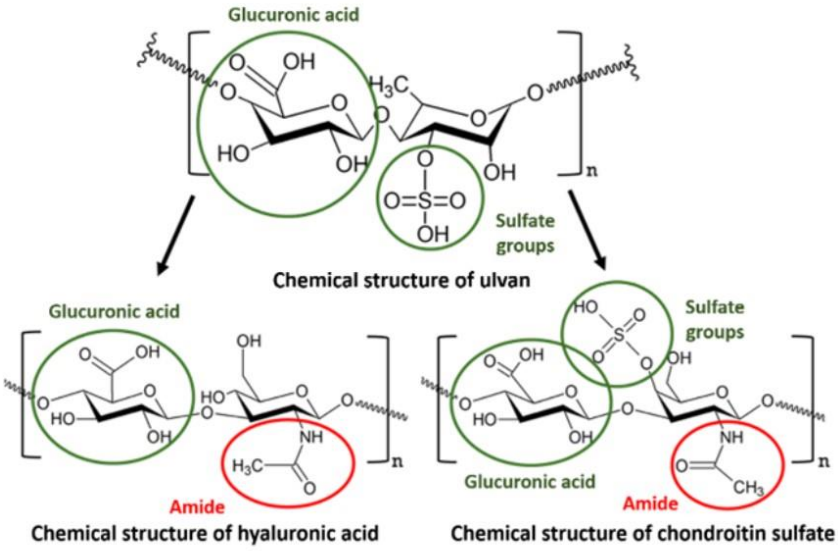


Figure 1: Chemical structure of ulvan, hyaluronic acid and chondroitin sulfate.

The bioactivity of sulfated polysaccharides is linked with their ability to interact with proteins, which is influenced by their chemical properties and molecular structure [24]. Therefore, sulfated polysaccharides can exhibit considerable heterogeneity in terms of molecular mass, sulfation pattern, and charge density. The use of ulvan for biomedical applications has several advantages, including the fact that this sulfated polysaccharide is bioavailable, can be obtained by a sustainable extraction process with low-cost production, shows structural similarities with fucoidan, chondroitin sulfate, and hyaluronic acid, and can be easily associated with other biopolymers by electrostatic interaction or carboxymethylation by the acid-catalyzed reaction [25, 26].

Bioactive sulfated polysaccharides with functional properties have been isolated from seaweeds, purified, characterized, and evaluated for biological applications. The primary focus of this study was to extract ulvan from *U. ohnoi* using an environmentally friendly technique based on suitable extraction and precipitation methods to assess its purity, enlarging the

potential of applications of the sulfated polysaccharides from seaweeds. The ulvan was morphologically and chemically characterized. The results unequivocally demonstrate that the achievement was reached, and that the suitable extraction method prove feasible involving fewer steps, resulting in high purity product, and being cost-effective.

Results and Discussion

The main aim of this study was to extract ulvan from *U. ohnoi* using an environmentally friendly technique based on suitable extraction and precipitation methods to assess its purity, enlarging the potential of applications of the sulfated polysaccharides from seaweeds. The macroscopic characteristics of dried *U. ohnoi* seaweed and ulvan are shown in Supplementary Material (**Figure S2**). **Figure S2.A** shows the macroscopic appearance of dried and standardized seaweed with a particle size of about 80 mesh. **Figure S2.B** shows that the lyophilized ulvan from the microwave-assisted extraction method (MAU-extraction) exhibits a flocculated structure of white color, with the absence of greenish pigments. Greenish pigments are regarded as impurities have origin in the extraction/purification process involving alkaline or acid solvents such as ammonium oxalate [$(NH_4)_2C_2O_4$] [40, 41] and hydrochloric acid (HCl) [42].

The elemental analysis by XRF to determine the crude protein content and total sulfate ions in the dry extract of ulvan is justified by the interest in evaluating the accuracy of the sulfate polysaccharide extraction method concerning the contents of these chemical elements [32, 36, 43]. The results for the elemental analysis of Carbon (C), Hydrogen (H), Nitrogen (N), sulfur (S), sulfate ions (SO_4), and total protein content in the ulvan samples are shown in **Table 1**. The sensitivity of this analytical method also makes it possible to measure the composition of the samples, as they may vary according to the algal species, seasonal collection periods, and conditions of the aquatic environment or the cultivation of algae [36, 44, 45]. Proteins in the cell walls of green algae are associated with polysaccharides. In this way, the protein content, especially the sulfated ones extracted with the polysaccharides, is considered impurities.

Table 1: Percentage (g/%) of carbon, hydrogen, nitrogen, sulfur, total protein, and sulphate for *U. ohnoi* and ulvan (experimental data) compared to previously reported data (literature data)

	Samples	Carbon	Hydrogen	Nitrogen	Sulfur	Protein	Sulphate	References
Experimental data	*Ulva ohnoi* (powdered dry seaweed)	24.48 ± 1.10	4.4 ± 0.24	1.38 ± 0.04	4.8 ± 0.63	6.88 ± 0.21	14.39 ± 1.89	n.a.
	Ulvan Microwave Assisted Aqueous Extraction	16.04 ± 0.20	3.84 ± 0.20	0.94 ± 0.04	8.32 ± 0.20	0.68 ± 0.18	24.97 ± 0.88	n.a.
Literature data	*Ulva ohnoi* (powdered dry seaweed)	27.00 ± 1.20	5.50 ± 0.10	3.70 ± 0.30	5.30 ± 0.10	18.50 ± 1.50	n.d	[46–48]
	Ulvan from *Ulva ohnoi* under acidic medium (HCl) and ultrafiltration	28.58 ± 0.02	4.83 ± 0.23	1.36 ± 0.12	5.74 ± 0.10	1.81 ± 0.10	17.60 ± 1.40	[42, 47]
	Ulvan from *Ulva ohnoi* in presence of $Na_2C_2O_4$ and ethanol	28.92 ± 0.30	4.66 ±0.11	3.43	3.6	5.90 ± 0.70	7.10 ± 0.70	[43, 46]
	Ulvan from *Ulva clathrate* hot water method	n.d	n.d	n.d	n.d	n.d	16.9	[49]
	Ulvan from *Ulva lactuca* dialysis and ethanol precipitation	29.23 ± 0.47	4.61 ± 0.29	2.04 ± 0.55	7.08 ± 0.26	3.27 ± 0.25	n.d	[50]

n.a., not applicable. n.d not determined

The amount of sulfate ions in various species of algae of the genus *Ulva* has been reported in the 2.3 to 40% range [49, 51] that, in turn, is associated with the molecular weight of ulvan and directly associated with bioactivity and with the characteristics of the polysaccharide group, including the chemical structure [36, 44, 52]. In the MAU-extraction method used in this study, the percentages of carbon, hydrogen, nitrogen, and total protein were lower than the values obtained when sodium oxalate [43, 46] was used in the extraction process. However, the amount of nitrogen, sulfur, and total proteins were higher than the values obtained when HCl [42, 47] was used for ulvan extraction. In contrast, the sulfate ion content was about three times higher when compared to the extraction method that used sodium oxalate, followed by ethanol precipitation [46], and about 1.5 times higher when compared to the extraction method having HCl as an extractor, followed by ultrafiltration [42]. These results show that the MAU-extraction method is more efficient, besides that faster and environmentally friendly when compared to other previously reported techniques for *U. ohnoi*. Additionally, as recently reported by Chen et al. [53], the content of sulfate ions obtained in this extraction process indicates that the molar mass of the ulvan, and consequently its antioxidant and anti-inflammatory bioactivities, are more significant than the ulvan obtained by the other aforementioned extraction techniques [43, 47, 48].

Free metallic elements act as counterion to ionizable radicals, such as sulfate, nitrate and phosphate groups. The sulfated polysaccharides found in green algae of the *Ulvales* genus are capable of accumulating trace elements of metals (~ 100μg/g), and therefore they must be investigated due to their importance from an environmental and public health point of view [54, 55]. To identify free metallic chemical elements potentially harmful, and other biologically active an X-ray fluorescence (XRF) was conducted.

The results shown in **Table 2** do not register the presence of any known harmful chemical elements including, heavy metals and others foreign to the molecular composition of ulvan. The free metallic chemical elements found in the samples of *U. ohnoi* and ulvan are probably from the aquatic environment in the region where the alga was raised and do not pose any danger to human health or ecosystems [56]. The absence of heavy metals reflects the marine ecosystem, which can be considered healthy, without harming fauna, flora and humans [56, 57]. In contrast, the presence of silicon is a relevant finding since this mineral element is a biological cross-linking agent and it also participates in the structure of connective tissues and plays an important role in initiating the bone calcification/mineralization process, by stimulating osteosynthesis by increasing collagen biosynthesis [58, 59].

Table 2: Free chemical elements present in *U. ohnoi* and ulvan.

Chemical elements	*U. ohnoi* (%)	Ulvan (%)
Sodium (Na, *natrium*)	Not detected	Not detected
Aluminium (Al)	Not detected	Not detected
Magnesium (Mg)	5.10 ± 0.02	1.09 ± 0.23
Calcium (Ca)	0.50 ± 0.03	0.78 ± 0.09
Potassium (K, *kallium*)	0.80 ± 0.10	1.77 ± 0.10
Silicon (Si)	0.30 ± 0.08	0.19 ± 0.02
Phosphorus (P)	0.04 ± 0.07	0.13 ± 0.03
Clorum (Cl)	0.30 ± 0.05	1.05 ± 0.23
Total	12.05 ± 0.12	5.01± 0.70

The yield from the MAU-extraction method was 27.77 ± 4.83%, which is about twice higher than the 13.88 ± 0.4% obtained when using ammonium oxalate and heating (80 °C, 2h). The differences in yield have been attributed to various factors in the ulvan extraction process, such as time, temperature, types of solvents, and methods [41]. The purity of the ulvan extracted from *U. ohnoi* by the MAU-extraction method was around 85%, which is a significant improvement compared to the purity ranging between 31% - 68% obtained using sulfuric acid (pH 1.0, 2.5, 4.0), different temperatures (40 °C, 65 °C, 90 °C), or various extraction times [35]. In addition to increasing yield, the MAU-extraction method decreased extraction time, reduced electricity consumption, and is more environmentally friendly than previously described methods [35, 60, 61]. Besides, the ulvan had a lower content of impurities, such as proteins (4.68 ± 0.18%) and ash (5.01 ± 0.70%), compared to the ulvan obtained in the extractive processes described by Glasson et al. [35] and Tsubaki et al. [60] who presented percentages of proteins in the range of 4.1 – 15% and ash in the range of 11.2 – 41.2% [30, 52, 60].

Figure 2 (a-b) illustrates the results of microscopic analyzes (SEM, HRTEM) and energy-dispersive X-ray spectroscopy in scanning TEM mode (EDX-STEM). These analyzes were performed to observe the ulvan morphology and texture as well as to determine the qualitative and quantitative elemental composition.

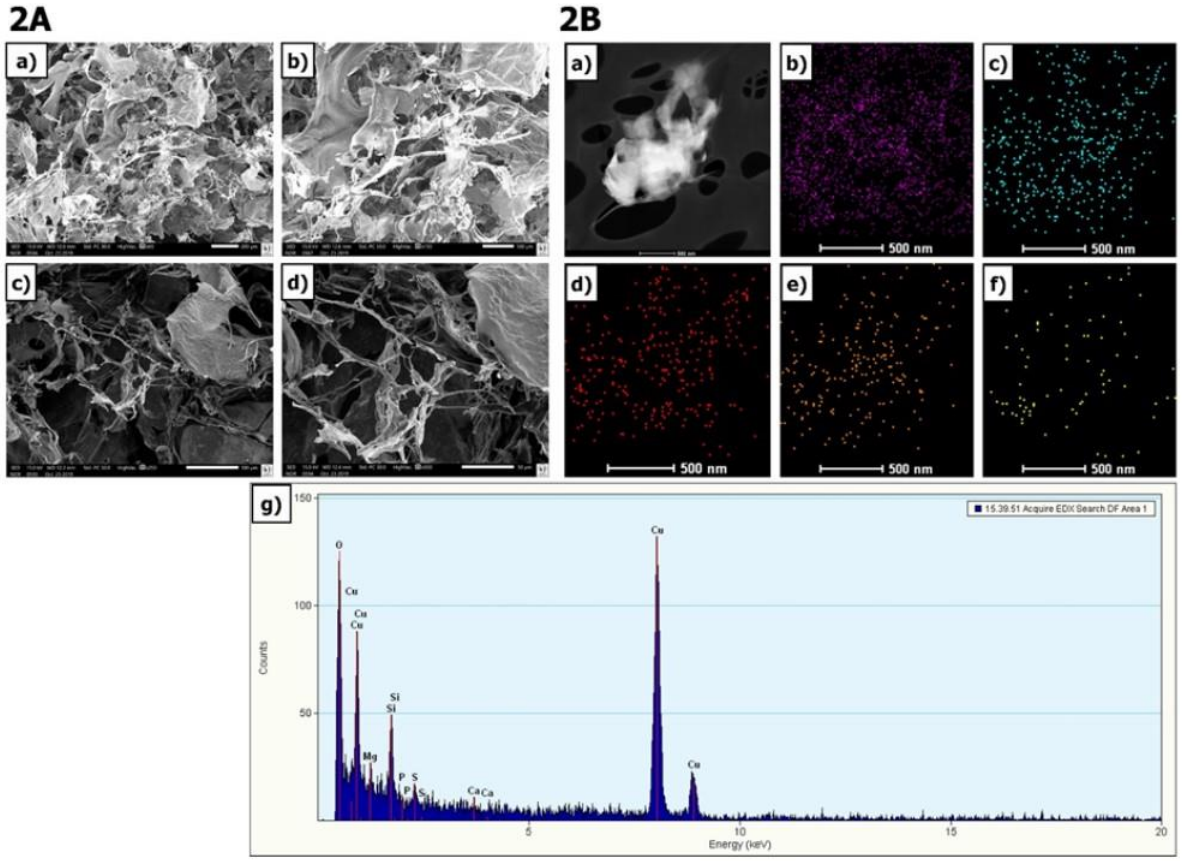


Figure 2: Micrographs captured by SEM and HRTEM. Panel 2A – By SEM at varying magnifications: a) 65x e 200 µm; b) 150x e 100 µm; c) 250x e 100 µm e d) 500x e 50 µm. Panel 2B – By HRTEM (a); elemental mapping of ulvan, where: oxygen – purple (b) | magnesium – turquoise (c) | sulfur – red (d) | phosphorus – orange (e) | calcium – yellow (f) and EDX spectrum of ulvan (g).

Figure 2A (a – d) shows the micrographs obtained by SEM. Images were randomly captured at distances between 200 and 50 nm and magnification factors of 65x, 150x, 250x, and 500x. The micrographs show the surface morphology of the fibers, filaments, and pores present in the ulvan structure. The surface morphology and the porosity of the fibers appear to be regularly shaped. So, the porous structure of ulvan suggests that it has a good swelling capacity; it can easily accommodate water-soluble or insoluble bioactive agents in this structure, like a scaffold, or make a gel and micro- and nanostructured systems and regulate the release of the active compound. Furthermore, the ulvan in thin film form could absorb a significant amount of exudate, contributing to wound healing [62]. The SEM micrographs of the ulvan did not show similarities with the SEM images reported in the previous study for the ulvan extracted from the seaweed *Ulva spp*. and *U. reticulata*, which showed a spongy-like structure without traces of fibers, pores, and filaments. The differences in the microscopic structure of ulvan may

be linked to the use of different species of green algae and the various extraction processes [41, 45, 56, 63]. In the HRTEM micrograph of the ulvan (**Figure 2B, a – f)**, it is possible to observe the presence of holes that ratify the pores in the fibers. The elemental mapping and the EDX spectrum shown in **Figure 2B (b – g**) indicate the presence of oxygen, magnesium, silicon, sulfur, phosphorus, and calcium in the structure of the ulvan, which corroborates with the results obtained in elemental analysis **(Table 1)** and X-ray fluorescence **(Table 2)**. According to the EDX results (**Figure 2B, g**), the ulvan sample analyzed showed 79.49% O, 7.48% Mg, 11.62% Si, 0.44% P, 0.95% S. These results are more promising for biomedical application of ulvan extracted from *U. ohnoi* than the results reported by Wahlström et al. [56] for ulvan extracted from *U. lactuca* and *U. compressa*.

The differences are probably related to the use of different algae, the extraction process, and the characteristics of the aquatic environment where the algae were collected [44, 56, 64]. The presence of oxygen and sulfur in the ulvan EDX spectrum comes from the chemical structure of the ulvan. While Ca, Mg, and P in ulvan are related to the presence of these elements in the environment. The presence of Si, in the form of SiO_2, comes from sea sand [56, 65]. The presence of copper (Cu) in the EDX spectrum comes from the copper mesh used for sample preparation in TEM [66].

The DSC method was employed in this study to assess the behavior of ulvan under controlled temperature increase and to evaluate the sample's thermal properties, such as melting temperature (Tm), glass transition (Tg), crystallization (Cry). The thermogram obtained by DSC for ulvan is shown in **Figure 3**.

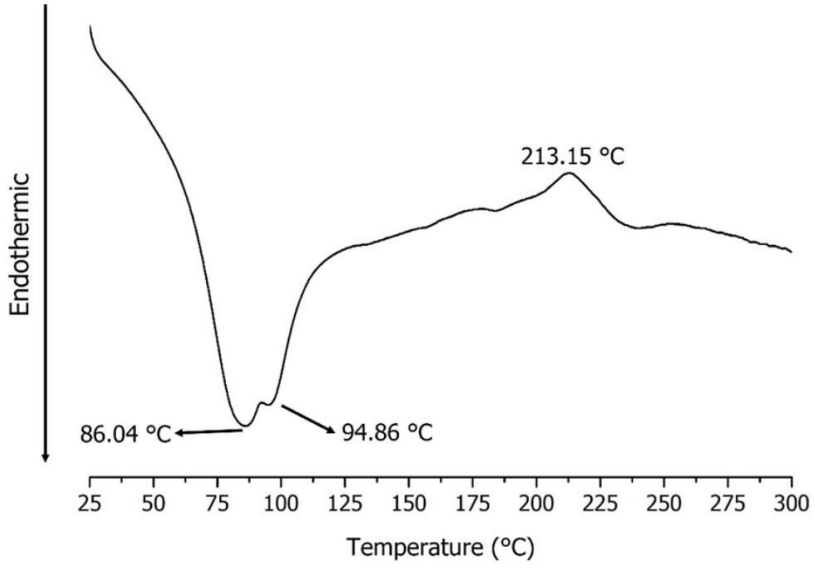


Figure 3: DSC thermogram of ulvan extracted of *U. ohnoi*.

Table 3 shows the results obtained for Mp events (86.04º C and 94.86º C) including onset, endset temperatures, an exothermic thermal of Cry at 213.15º C, and the enthalpies (ΔH) of fusion (213.01 ºC) and Cry (+ 26.28 ºC), and discreet Tg event (0,08 mW/mg) between 174.08 °C and 180.74 °C that is poorly defined due to the high crystallinity degree. The Cry peak is a typical feature of polysaccharides that occurs to some extent if a molecule has a sufficiently regular structure. The ulvan thermal events observed in this study differ from another one previously reported DSC for the ulvan from the seaweed *U. rigida*, which showed a broad endothermic melting event at 105.4 °C and an exothermic degradation event at 227.7 °C [67]. Then, it is further evidence that the different species of green algae or extraction methods modify the ulvan properties.

Table 3. Thermal properties of ulvan from *Ulva Ohnoi*.

Sample	Peaks	Onset (°C)	Mp (°C)	CRY (°C)	Endset (°C)	ΔH (J/g)
Ulvan	1	66.68	86.04	-	108.72	-231.01
	2	92.33	94.86	-	101.08	-4.96
	3	204.20	-	213.15	230.26	+26.28

The thermogram is typical of a semicrystalline substance since it presents endothermic and exothermic events and discreet Tg (0,08 mW/mg). The endothermic event at 174.08 – 184 ºC also differs from the other reported results for the ulvan extracted from the seaweed *U. armoricana* [37, 68]. The presence of the endothermic events at 86.04 ºC and 94.86 ºC are related to the ulvan and evaporation of free water present in the sample, respectively [69, 70]. These results corroborate the analysis of the DSC results previously reported by since, according to these authors, a broad endothermic event indicates the presence of several substances, while an endothermic sharp melting event characterizes samples of the pure polysaccharides [37, 69, 70]. Compared to chondroitin sulfate, ulvan showed differences in the endothermic and exothermic events [71]. These results can be explained by the differences in the molar weight of ulvan and chondroitin sulfate and the presence of impurities [71–75].

FTIR was used to characterize and identify characteristic chemical groups of ulvan [62, 76]. The spectrogram obtained by FTIR for the ulvan is shown in **Figure 4**.

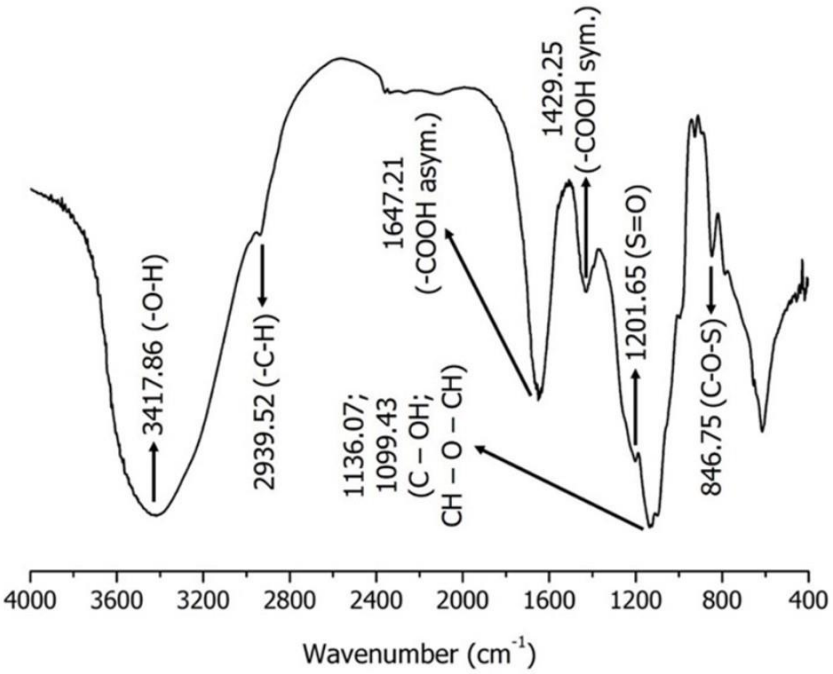


Figure 4: FTIR spectrogram of the ulvan extracted from *Ulva ohnoi*.

Analysis of the results obtained for ulvan show a band at 3417.86 cm^{-1} that is attributed to hydroxyl groups (– OH), the peak at 2939.52 cm^{-1} corresponds to the stretching of the –CH bond, the peak at 1647.21 cm^{-1} corresponds to the asymmetric stretching of the carboxylic groups (–COOH) present in uronic acids. The peak 1429.25 cm^{-1} corresponds to the symmetrical stretching of the carboxylic groups (–COOH) and the stretching of the C–OH bond that belongs to the –COOH groups [49, 76]. The peak displayed at 1201.65 cm^{-1} corresponds to the stretching of the S = O bond of the sulfate groups (RO– SO3-) present in the chemical structure of ulvan, the peaks at 1136.07 cm^{-1} and 1099.43 cm^{-1} correspond to the stretching of the C bonds – OH and HC– O– CH corresponding to the glycosidic ether, and the peak at 846.75 cm^{-1} corresponds to the flexural stretching of the C– O – S bond of the sulfate groups in the axial position [76, 77].

The ulvan FTIR spectrogram presents chemical similarities with chondroitin sulfate and hyaluronic acid, except in the stretch that corresponds to the amide group (1653-1636 cm^{-1}), since this group is not present in the chemical structure of ulvan (**Figure 1**) [78, 79].

The ^{1}HNMR technique was performed in order to study the chemical structure of ulvan in more detail [36, 37]. In the ^{1}H NMR spectrum of ulvan (**Figure 5**), the hydrogen chemical shifts at 4.65 ppm, in the range of 3.51 – 3.53 ppm and in the range of 3.31 – 3.34 ppm refer to glucuronic acid, the shifts in 4.67 ppm, 3.98 ppm and 3.51 ppm refer to iduronic acid, the shifts

at 4.12 ppm and 3.63 ppm refer to sulfated rhamnose and the shifts at 2.78 ppm and in the range of 1.03 – 1.20 ppm refer to the methyl group (-CH_3) present in sulfated rhamnose [36, 49, 69].

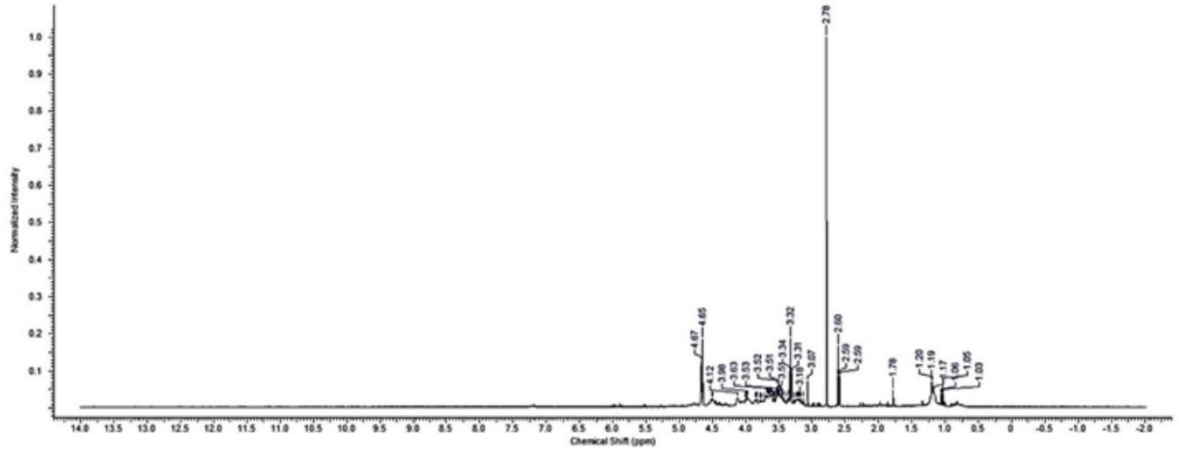


Figure 5: ^{1}H NMR spectrogram of the ulvan from *Ulva ohnoi*.

Thus, the ^{1}H NMR spectrum of ulvan presents similarities with the ^{1}H NMR spectra of hyaluronic acid, and chondroitin sulfate found in the literature since the spectra of the three polymers present chemical shifts corresponding to the glucuronic acid; however, the ulvan showed differences in the intensity and positioning of these displacements, which are related to differences in the chemical structures of these polymers, since, instead of presenting sulfated rhamnose in its polymeric chain, hyaluronic acid and chondroitin sulfate present the monosaccharides N-acetylglucosamine and N-acetyl-β-galactosamine-4-sulfate, respectively. Furthermore, differences in the intensity of chemical shifts may be related to differences in molar masses and chain sizes of these three polymers [80, 81].

XRD was performed in order to determine the degree of crystallinity and the main crystalline reflections of the ulvan [69]. The XRD diffractogram obtained for the ulvan is shown in **Figure 6**, in which the crystalline reflections at 16.1°, 18.4°, 20.3°, 22°, 24.8°, 28.2°, 30.6°, 32.2°, 35.7°, 39.5°, 45.5° and 48.7° are notable.

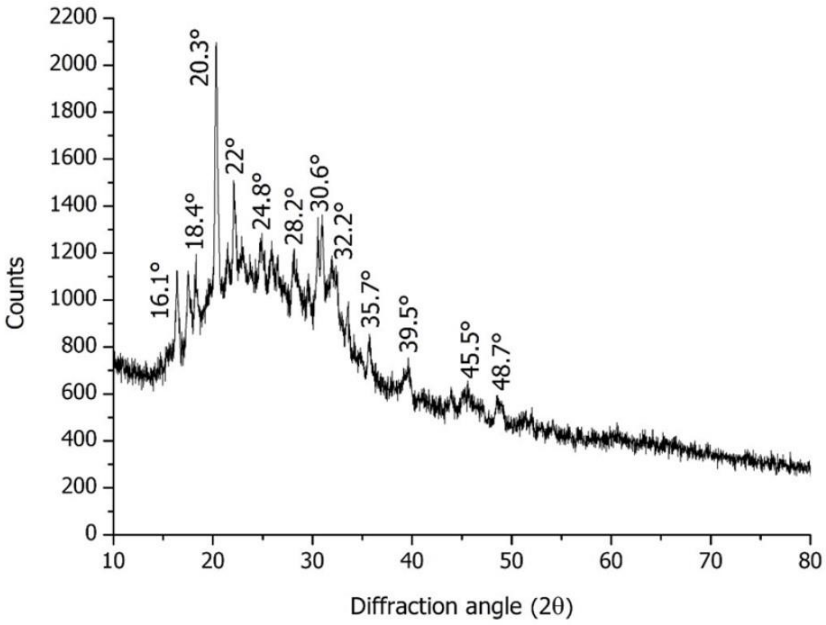


Figure 6: XRD diffractogram of ulvan from *Ulva ohnoi*.

From this diffractogram, it was determined that the ulvan obtained in this study presents a degree of crystallinity of 38%, which characterizes a semi-crystalline polymer, since the diffractogram of this sulfated polysaccharide presented a region of peaks characteristic of crystalline substances and an amorphous region predominant [34, 82]. The differences between the ulvan diffractogram and the chondroitin sulfate and sodium hyaluronate diffractograms can be explained by differences in the chemical structures and molar weight of these polymers since the crystallinity of the polymers is directly related to these factors [83, 84].

The present study aimed to extract ulvan from *U. ohnoi* using an environmentally friendly technique, focusing on the yield and purity of this important sulfated polysaccharide. We used a range of characterization techniques, exceptionally high-resolution microscopy, to investigate the structural properties of ulvan that would justify its use for drug delivery and other biomedical applications. Due to the chemical similarity and structure of ulvan with hyaluronic acid, and following its example, we envision the possibility of ulvan serving as a monoclonal antibody transporter via overexpression of M cells in Peyer's patches, which are connected to the mesenteric lymph nodes [18]. From the sulfate ion, we evaluated the use of ulvan for the graphitization of the nanoparticulate systems (studies not yet published). The anti-biofilm activity of sulfated polysaccharides has been reported [22], as well as antibacterial activity [85]. Despite the few studies reporting the use of ulvan for medicinal purposes, we believe that ulvan extracted from green macroalgae, especially from the genus *Ulva* and

particularly of the macroalgae *U. ohnoi*, can now be recognized as a platform for conducting various biomedical studies. The ongoing efforts hold promise for the future of genus *Ulva* and its potential biomedical applications, including vaccines for nasal administration and target-specific systems, among other smart drug delivery systems.

Conclusions

A bioactive sulfated polysaccharide was obtained through suitable extraction and precipitation using an environmentally friendly method free of acid or alkaline solvents, involves fewer steps, results in high purity, and is cost-effective with potential to be commercially explored. The experimental differences observed in ulvan properties, which are likely influenced by the use of different algae and extraction methods, and the unique characteristics of this polysaccharide, as well as its potential for biomedical use, underscore the novelty and importance of our research.

Our studies demonstrate that the aqueous extraction process assisted by microwave energy, followed by ethanol precipitation, efficiently obtained the ulvan with high yield and purity. The porous nature of ulvan supported by sulfated polysaccharide fibers reveals various possibilities for transporting and releasing drugs, macromolecules, and antigens. In addition to the reported bacterial activity, the sulfated polysaccharides can be beneficial for the manufacture of scaffolds intended for tissue regeneration and wound healing. The presence of mineral elements in the dry extract of ulvan is natural and is linked to the marine microenvironment at the time of seaweed collection. We investigated and demonstrated that the ulvan samples obtained are free of heavy metals, an important finding when dealing with algae of the Ulvaceae family.

On the other hand, the presence of Si identified in the extract can be seen as positive since it contributes to the increase of collagen biosynthesis, as one of the main constituents of the extracellular matrix, an important element in the regeneration of organic tissues, especially bone tissue. Furthermore, due to the presence of mineral salts, the biomass of the *U. ohnoi* plant or extract has been investigated as an alternative supplement that supports nutrition and promotes vegetative growth of plants grown in soil poor in mineral nutrients [86]. Due to the different applications, the dried plant and the *U. ohnoi* extract should be seen as a platform for studies to use better the marine biomass of this macroalgae and others of the order Ulvales (Chlorophyta).

MATERIALS and METHODS

Materials

Seaweed *U. ohnoi* (dried and without residual moisture) was kindly donated by the Laboratory of Phycology (LAFIC) of the Federal University of Santa Catarina (UFSC), campus of

Florianópolis – Santa Catarina – Brazil. Absolute ethanol PA was obtained from Synth (Diadema, São Paulo, Brazil – Batch: 226903).

Ulvan extraction and chemical characterization

For ulvan extraction, the previously described procedures [27–29] were used with modifications to increase yield and reduce extraction time. A flowchart with the main stages of the extraction process is shown in Supplementary Material (**Figure S1)**. Briefly, the dried seaweed was crushed in a knife mill (model O35, Marconi, Piracicaba, Brazil) to a granulometry corresponding to 80 mesh (180 µm). The seaweed powder was dispersed (1: 36) in purified water over 60 min. The obtained dispersion was subjected to homogenization (Ultra-Turrax, T 25 D S32, IKA, Staufen, Germany) with constant stirring (3,400 rpm/ 10 min.). The aqueous dispersion was heated in a microwave oven (BMS45A, Brastemp, São Paulo, Brazil) for 30s with an average power of 420 W. Then, the dispersion was filtered through filter paper with a vacuum aid. The residue retained on the filter paper was dried in an oven with forced air circulation at 35º C (TE-394/2, TECNAL, Piracicaba, Brazil) and stored for further analysis. The aqueous extract was mixed with ethanol (1: 3) and quickly refrigerated to precipitate the ulvan (-75 ± 5° C, 2 h). The precipitate was concentrated by removing the ethanol using a rotatory evaporator (45 ± 1° C, -600 mmHg). The concentrated aqueous dispersion was frozen (-75 ± 5° C) for 24 h and lyophilized (Freeze-drier - L101, Liotop, São Paulo, Brazil). The dried extracts were then stored in a packing hermetically closed and protected from light.

Scanning electron microscopy

To perform the scanning electron microscopy (SEM) technique, a sample of the ulvan was placed on an adhesive carbon tape, fixed to an aluminum support and covered with a thin layer of gold ions (DII-29010SCTR Smart Coater, JEOL, Tokyo, Japan). The sample was randomly microphotographed in SEM (JSM-IT200, JEOL, Tokyo, Japan), with an interference voltage of 15 kV.

Transmission electron microscopy

To perform the high-resolution transmission electron microscopy (HRTEM) technique, a sample of ulvan was dispersed in water and properly homogenized in an ultrasound bath (40 kHz, 1 h). A drop of the dispersion was placed on an ultrafine copper grid with Lacey carbon mesh film, 400 mesh, and subject to water evaporation at room temperature. The morphological characteristics of the ulvan were analyzed in HRTEM (FEI / TECNAI G2 F20) with an accelerating voltage of 200 kV. Simultaneously, to characterize the main chemical elements present in ulvan, energy dispersive X-ray spectroscopy (EDX) was performed in scanning transmission electron microscopy (STEM) mode [30].

Protein and sulfate ion contents

To determine the percentages of carbon (C), hydrogen (H), nitrogen (N) and sulfur (S) present in ulvan, an elemental analysis by combustion was performed (FlashSmart, Thermo-Scientific, Massachusetts, USA). A sample of ulvan (4 mg) was heated to a temperature of 950° C and held for 12 minutes [31]. The test was performed in triplicate. The percentage of proteins in the ulvan was calculated from the nitrogen (N%) content, following the Dumas method. This method determined the total protein content present in the ulvan based on the nitrogen conversion factor for both *U. ohnoi* and ulvan [31–33]. The total protein content present in ulvan was calculated (Equation 1). Data were expressed in percentage of dry mass (n=3).

$$Protein\ content\ \%(w/w) = N\ \times\ 5/100 \qquad eq.1$$

where *w/w* represents mass/mass percentage, "*N"* is the nitrogen content and "*5*" is the conversion factor for protein determination. The result of the elemental analysis for S was used to determine the content of sulfate ions (SO_4^{2-}) present in the ulvan. This content was determined based on the percentage of sulfur (%S) present in the sample and the S conversion factor (factor 3) [34]. Thus, the sulfate ion content of ulvan was calculated (Equation 2). Data were expressed in percentage of dry mass (w/w), n=3.

$$Sulfate\ content\ (\%) = S\ \times\ 3\ /100 \qquad eq.2$$

where "*S*" is the sulfur content, and "*3*" is the conversion factor for sulfate ions determination.

X-ray fluorescence

The X-ray fluorescence (XRF) technique was used to identify the main metallic and non-metallic chemical elements present in the ulvan sample and to determine their respective atomic concentrations. To carry out this technique, a tablet composed of ulvan and cellulose (1:8) was prepared, which was analyzed in an XRF spectrometer (Ɛpsilon 1, PANalytical, Almelo, Holland) equipped with a silver anode (Ag) and the results were obtained with the Ɛpsilon 3 software.

Yield and purity

The yield of the ulvan extraction process was calculated based on the dry mass of *U. ohnoi* and the mass of freeze-dried ulvan (**Equation 3**). Data were expressed in percentage of dry mass (w/w).

$$Ulvan\ yield\ (\%) = \frac{Mass\ of\ lyophilized\ ulvan\ \ (g)}{Dry\ mass\ of\ Ulva\ ohnoi\ (g)} \times 100 \qquad eq.3$$

For the calculation of the polysaccharide mass yield, the masses relative to impurities determined in the X-ray fluorescence assays were disregarded (protein content and other

chemical elements that are not part of the ulvan polymeric chain) [35, 36]. The impurity-free ulvan mass and percentage of purity was calculated using Equation 4 and Equation 5, respectively.

$$\text{Ulvan I}f\ (g) = Ulvan\ T\ (g) - \ TIc\ (g) \qquad eq.4$$

$$Ulvan\ purity\ (\%) = \frac{Ulvan\ If\ (g)}{Ulvan\ T\ \ (g)} \times 100 \qquad eq.5$$

Ulvan-If is the amount of ulvan free impurities, Ulvan-T is the amount of ulvan, and TI-c is the total impurity content.

Differential scanning calorimetry

The ulvan thermogram was obtained by the differential scanning calorimetry (DSC) technique (Thermal Analyzer TA 60W – Shimadzu, DSC-60, Kyoto, Japan). For this, a mass of approximately 3 mg of ulvan was transferred to an aluminum crucible, which was hermetically closed. Heating was carried out at a temperature range of 25 to 300 ºC, under a dynamic nitrogen (N_2) atmosphere and a flow rate of 50 mL/min, and a heating rate of 10 °C/min.

2.1. Fourier transform infrared spectroscopy

The ulvan was characterized by Fourier Transform Infrared (FTIR) spectroscopy (IRAffinity-1S, Shimadzu, Kyoto, Japan and Software LabSolutions v.2.10) in transmittance mode, using a KBr chip, in the wavelength range of 4000 – 400 cm^{-1}, after 64 scans, and resolution of 4 cm^{-1}. Spectrograms were normalized, and vibration band assignment was carried out in the IR spectra of samples by comparing the position, relative intensity, or shape of the bands associated with the main chemical groups found in the sulfated polysaccharides with the corresponding features of the associated functional group bands.

Nuclear resonance magnetic spectroscopy

To perform hydrogen-1 nuclear magnetic resonance (^{1}H NMR) spectroscopy, ulvan dispersion was prepared in the presence of deuterium oxide (D_2O) with a high degree of purity (99.9%). The sample (10 mg) was dispersed and homogenized in 700 µL of D_2O, which was placed in NMR tubes with a diameter of 5 mm. The ^{1}H NMR technique was performed using a nuclear magnetic resonance spectrometer (500/54 Premium Shielded, Agilent Technologies, California, USA) with a proton frequency of 500 MHz and a temperature of 25° C. The ^{1}H NMR spectrum of the ulvan was recorded with a pulse width of 8 µs, acquisition time of 4.089 s, relaxation delay of 2 s and 256 transients. Spectral width ranged from 2 to +14 ppm [37].

X-ray diffraction

The ulvan was analyzed in an X-ray diffractometer (D8 advance, Bruker, Massachusetts, USA) with a position-sensitive detector (LinxEve) and with a Cu-Kα radiation source (λ = 1.5418 Å).

XRD data were recorded in the range of 10° < 2θ < 80° with a step of 0.02° and irradiation time of 0.5 s per step [38]. The degree of crystallinity of this sulfated polysaccharide was determined by calculating the ratio of the crystalline area corresponding to the peaks to the total area of the diffractogram, as shown in Equation 6. The total area of the diffractogram was calculated using the OriginPro 8.5 software after the line correction baseline [39]. The crystallinity degree was expressed in percentage (%).

$$Crystallinity\ degree\ \ (\%) = \frac{Crystalline\ area}{Total\ area} \times 100 \qquad eq.6$$

Data availability statements

All data generated or analysed during this study are included in this published article and its supplementary information files.

Declaration of competing interest

The authors declare that no competing financial interests influence the work reported in this paper.

Acknowledgements

Marco V. Chaud acknowledges the support received São Paulo Research Foundation (FAPESP, São Paulo, Brazil) (Process number 2018/11350-6). Coordination for the Improvement of Higher Education Personnel (PROSUC/CAPES) (Process Number 88887.178181/2018-00) for granting a scholarship. Laboratory of Applied Nuclear Physics of the University of Sorocaba (LAFINAU). Laboratory of Biomaterials and Nanotechnology of UNISO (LaBNUS). Laboratory of Structural Characterization (LCE/DEMa/UFSCar). Eliana B. Souto acknowledges the support received from national funds from FCT—Fundação para a Ciência e a Tecnologia, I.P., in the scope of the project UIDP/04378/2020 and UIDB/04378/2020 of the Research Unit on Applied Molecular Biosciences—UCIBIO and the project LA/P/0140/2020 of the Associate Laboratory Institute for Health and Bioeconomy—i4HB.

References

1. Allmendinger A, Spavieri J, Kaiser M, et al (2010) Antiprotozoal, antimycobacterial and cytotoxic potential of twenty-three British and Irish red algae. Phyther Res 24:1099–1103. https://doi.org/10.1002/ptr.3094
2. Shah SAA, Hassan SS ul, Bungau S, et al (2020) Chemically Diverse and Biologically Active Secondary Metabolites from Marine Phylum chlorophyta. Mar Drugs 18:493. https://doi.org/10.3390/md18100493

3. Ammar EE, Aioub AAA, Elesawy AE, et al (2022) Algae as Bio-fertilizers: Between current situation and future prospective. Saudi J Biol Sci 29:3083–3096. https://doi.org/10.1016/j.sjbs.2022.03.020

4. Li S, Show PL, Ngo HH, Ho S-H (2022) Algae-mediated antibiotic wastewater treatment: A critical review. Environ Sci Ecotechnology 9:100145. https://doi.org/10.1016/j.ese.2022.100145

5. Pankiewicz R, Łęska B, Messyasz B, et al (2016) First isolation of polysaccharidic ulvans from the cell walls of freshwater algae. Algal Res 19:348–354. https://doi.org/10.1016/j.algal.2016.02.025

6. Bastos E, Schneider M, de Quadros DPC, et al (2019) Phytoremediation potential of Ulva ohnoi (Chlorophyta): Influence of temperature and salinity on the uptake efficiency and toxicity of cadmium. Ecotoxicol Environ Saf 174:334–343. https://doi.org/10.1016/j.ecoenv.2019.01.130

7. Steinhagen S, Barco A, Wichard T, Weinberger F (2019) Conspecificity of the model organism Ulva mutabilis and Ulva compressa (Ulvophyceae, Chlorophyta). J Phycol 55:25–36. https://doi.org/10.1111/jpy.12804

8. Hiraoka M, Shimada S, Uenosono M, Masuda M (2004) A new green-tide-forming alga, Ulva ohnoi Hiraoka et Shimada sp. nov. (Ulvales, Ulvophyceae) from Japan. Phycol Res 52:17–29. https://doi.org/10.1111/j.1440-1835.2003.00321.x

9. Neori A, Bronfman Y, van Rijn J, et al (2020) The suitability of Ulva fasciata, Ulva compressa, and Hypnea musciformis for production in an outdoor spray cultivation system, with respect to biomass yield and protein content. J Appl Phycol 32:3183–3197. https://doi.org/10.1007/s10811-020-02130-3

10. Bastos E, Gouvêa LP, Horta PA, Rörig LR (2019) Interaction between salinity and phosphorus availability can influence seed production of Ulva ohnoi (Chlorophyta, Ulvales). Environ Exp Bot 167:103860. https://doi.org/10.1016/j.envexpbot.2019.103860

11. Mata L, Magnusson M, Paul NA, de Nys R (2016) The intensive land-based production of the green seaweeds Derbesia tenuissima and Ulva ohnoi: biomass and bioproducts. J Appl Phycol 28:365–375. https://doi.org/10.1007/s10811-015-0561-1

12. Fernández-Díaz C, Coste O, Malta E (2017) Polymer chitosan nanoparticles functionalized with Ulva ohnoi extracts boost in vitro ulvan immunostimulant effect in Solea senegalensis macrophages. Algal Res 26:135–142. https://doi.org/10.1016/j.algal.2017.07.008

13. He C, Muramatsu H, Kato S, Ohnishi K (2017) Characterization of an Alteromonas long-type ulvan lyase involved in the degradation of ulvan extracted from Ulva ohnoi. Biosci Biotechnol Biochem 81:2145–2151. https://doi.org/10.1080/09168451.2017.1379352

14. Morelli A, Betti M, Puppi D, et al (2016) Enzymatically Crosslinked Ulvan Hydrogels as Injectable Systems for Cell Delivery. Macromol Chem Phys 217:581–590. https://doi.org/10.1002/macp.201500353

15. Tziveleka L, Ioannou E, Roussis V (2019) Ulvan, a bioactive marine sulphated polysaccharide as a key constituent of hybrid biomaterials: A review. Carbohydr

Polym 218:355–370. https://doi.org/10.1016/j.carbpol.2019.04.074

16. Yıldırım S, Özener HÖ, Doğan B, Kuru B (2018) Effect of topically applied hyaluronic acid on pain and palatal epithelial wound healing: An examiner-masked, randomized, controlled clinical trial. J Periodontol 89:36–45. https://doi.org/10.1902/jop.2017.170105

17. Pilloni A, Schmidlin PR, Sahrmann P, et al (2019) Effectiveness of adjunctive hyaluronic acid application in coronally advanced flap in Miller class I single gingival recession sites: a randomized controlled clinical trial. Clin Oral Investig 23:1133–1141. https://doi.org/10.1007/s00784-018-2537-4

18. de Souza AB, Chaud MV, Alves TF, et al (2020) Hyaluronic acid in the intestinal tract: Influence of structure, rheology, and mucoadhesion on the intestinal uptake in rats. Biomolecules 10:1422. https://doi.org/10.3390/biom10101422

19. Tran TT Van, Truong HB, Tran NHV, et al (2018) Structure, conformation in aqueous solution and antimicrobial activity of ulvan extracted from green seaweed Ulva reticulata. Nat Prod Res 32:2291–2296. https://doi.org/10.1080/14786419.2017.1408098

20. Massironi A, Morelli A, Grassi L, et al (2019) Ulvan as novel reducing and stabilizing agent from renewable algal biomass: Application to green synthesis of silver nanoparticles. Carbohydr Polym 203:310–321. https://doi.org/10.1016/j.carbpol.2018.09.066

21. Zhong H, Gao X, Cheng C, et al (2020) The Structural Characteristics of Seaweed Polysaccharides and Their Application in Gel Drug Delivery Systems. Mar Drugs 18:658. https://doi.org/10.3390/md18120658

22. Gadenne V, Lebrun L, Jouenne T, Thebault P (2013) Antiadhesive activity of ulvan polysaccharides covalently immobilized onto titanium surface. Colloids Surfaces B Biointerfaces 112:229–236. https://doi.org/10.1016/j.colsurfb.2013.07.061

23. Wang D-A, Varghese S, Sharma B, et al (2007) Multifunctional chondroitin sulphate for cartilage tissue-biomaterial integration. Nat Mater 6:385–392. https://doi.org/10.1038/nmat1890

24. Valcarcel J, García MR, Sampayo LF, Vázquez JA (2020) Marine chondroitin sulfate of defined molecular weight by enzymatic depolymerization. Carbohydr Polym 229:115450. https://doi.org/10.1016/j.carbpol.2019.115450

25. Don T-M, Liu L-M, Chen M, Huang Y-C (2021) Crosslinked complex films based on chitosan and ulvan with antioxidant and whitening activities. Algal Res 58:102423. https://doi.org/10.1016/j.algal.2021.102423

26. Mariia K, Arif M, Shi J, et al (2021) Novel chitosan-ulvan hydrogel reinforcement by cellulose nanocrystals with epidermal growth factor for enhanced wound healing: In vitro and in vivo analysis. Int J Biol Macromol 183:435–446. https://doi.org/10.1016/j.ijbiomac.2021.04.156

27. Pengzhan Y, Quanbin Z, Ning L, et al (2003) Polysaccharides from Ulva pertusa (Chlorophyta) and preliminary studies on their antihyperlipidemia activity. J Appl Phycol 15:21–27. https://doi.org/10.1023/A:1022997622334

28. Cluzet S, Torregrosa C, Jacquet C, et al (2004) Gene expression profiling and

protection of Medicago truncatula against a fungal infection in response to an elicitor from green algae Ulva spp. Plant, Cell Environ 27:917–928. https://doi.org/10.1111/j.1365-3040.2004.01197.x

29. Paulert R, Talamini V, Cassolato JEF, et al (2009) Effects of sulfated polysaccharide and alcoholic extracts from green seaweed Ulva fasciata on anthracnose severity and growth of common bean (Phaseolus vulgaris L.). J Plant Dis Prot 116:263–270. https://doi.org/10.1007/BF03356321

30. González-Ballesteros N, Rodríguez-Argüelles MC, Prado-López S, et al (2019) Macroalgae to nanoparticles: Study of Ulva lactuca L. role in biosynthesis of gold and silver nanoparticles and of their cytotoxicity on colon cancer cell lines. Mater Sci Eng C 97:498–509. https://doi.org/10.1016/j.msec.2018.12.066

31. Mæhre HK, Dalheim L, Edvinsen GK, et al (2018) Protein Determination — Method Matters. Foods 7:5. https://doi.org/10.3390/foods7010005

32. Kidgell JT, Glasson CRK, Magnusson M, et al (2020) The molecular weight of ulvan affects the in vitro inflammatory response of a murine macrophage. Int J Biol Macromol 150:839–848. https://doi.org/10.1016/j.ijbiomac.2020.02.071

33. Laurens LML, Olstad JL, Templeton DW (2020) Total Protein Content Determination of Microalgal Biomass by Elemental Nitrogen Analysis and a Dedicated Nitrogen- to-Protein Conversion Factor. In: Spilling K (ed) Biofuels from Algae. Humana, New York, NY, pp 233–242

34. Gajaria TK, Bhatt H, Khandelwal A, et al (2020) A facile chemical cross- linking approach toward the fabrication of a sustainable porous ulvan scaffold. J Bioact Compat Polym 35:301–313. https://doi.org/10.1177/0883911520939986

35. Glasson CRK, Donnet L, Angell A, et al (2019) Multiple response optimisation of the aqueous extraction of high quality ulvan from Ulva ohnoi. Bioresour Technol Reports 7:100262. https://doi.org/10.1016/j.biteb.2019.100262

36. Sari-Chmayssem N, Taha S, Mawlawi H, et al (2019) Extracted ulvans from green algae Ulva linza of Lebanese origin and amphiphilic derivatives: evaluation of their physico-chemical and rheological properties. J Appl Phycol 31:1931–1946. https://doi.org/10.1007/s10811-018-1668-y

37. Yaich H, Amira A Ben, Abbes F, et al (2017) Effect of extraction procedures on structural, thermal and antioxidant properties of ulvan from Ulva lactuca collected in Monastir coast. Int J Biol Macromol 105:1430–1439. https://doi.org/10.1016/j.ijbiomac.2017.07.141

38. He J, Li J, Du W, et al (2018) A mesoporous metal-organic framework: Potential advances in selective dye adsorption. J Alloys Compd 750:360–367. https://doi.org/10.1016/j.jallcom.2018.03.393

39. Espino-Pérez E, Gilbert RG, Domenek S, et al (2016) Nanocomposites with functionalised polysaccharide nanocrystals through aqueous free radical polymerisation promoted by ozonolysis. Carbohydr Polym 135:256–266. https://doi.org/10.1016/j.carbpol.2015.09.005

40. Li W, Wang K, Jiang N, et al (2018) Antioxidant and antihyperlipidemic activities of purified polysaccharides from Ulva pertusa. J Appl Phycol 30:2619–2627.

https://doi.org/10.1007/s10811-018-1475-5

41. Prabhu MS, Israel A, Palatnik RR, et al (2020) Integrated biorefinery process for sustainable fractionation of Ulva ohnoi (Chlorophyta): process optimization and revenue analysis. J Appl Phycol 32:2271–2282. https://doi.org/10.1007/s10811-020-02044-0

42. Glasson CRK, Luiten CA, Carnachan SM, et al (2022) Structural characterization of ulvans extracted from blade (Ulva ohnoi) and filamentous (Ulva tepida and Ulva prolifera) species of cultivated Ulva. Int J Biol Macromol 194:571–579. https://doi.org/10.1016/j.ijbiomac.2021.11.100

43. Yaich H, Garna H, Besbes S, et al (2013) Effect of extraction conditions on the yield and purity of ulvan extracted from Ulva lactuca. Food Hydrocoll 31:375–382. https://doi.org/10.1016/j.foodhyd.2012.11.013

44. Yaich H, Garna H, Besbes S, et al (2014) Impact of extraction procedures on the chemical, rheological and textural properties of ulvan from Ulva lactuca of Tunisia coast. Food Hydrocoll 40:53–63. https://doi.org/10.1016/j.foodhyd.2014.02.002

45. Thu QTM, Luong DV, Nu NT, et al (2016) Effect of Sulfation on the Structure and Anticoagulant Activity of Ulvan Extracted From Green Seaweed Ulva Reticulata. Vietnam J Sci Technol 54:373–379. https://doi.org/10.15625/2525-2518/54/2c/11863

46. Glasson CRK, Sims IM, Carnachan SM, et al (2017) A cascading biorefinery process targeting sulfated polysaccharides (ulvan) from Ulva ohnoi. Algal Res 27:383–391. https://doi.org/10.1016/j.algal.2017.07.001

47. He J, Xu Y, Chen H, Sun P (2016) Extraction, Structural Characterization, and Potential Antioxidant Activity of the Polysaccharides from Four Seaweeds. Int J Mol Sci 17:1988. https://doi.org/10.3390/ijms17121988

48. Ibrahim MIA, Amer MS, Ibrahim HAH, Zaghloul EH (2022) Considerable Production of Ulvan from Ulva lactuca with Special Emphasis on Its Antimicrobial and Anti-fouling Properties. Appl Biochem Biotechnol 194:3097–3118. https://doi.org/10.1007/s12010-022-03867-y

49. Chi Y, Li H, Wang P, et al (2020) Structural characterization of ulvan extracted from Ulva clathrata assisted by an ulvan lyase. Carbohydr Polym 229:115497. https://doi.org/10.1016/j.carbpol.2019.115497

50. Maray SO, Abdel-Kareem MSM, Mabrouk MEM, et al (2023) In Vitro Assessment of Antiviral, Antimicrobial, Antioxidant and Anticancer Activities of Ulvan Extracted from the Green Seaweed Ulva lactuca. Thalass An Int J Mar Sci 39:779–790. https://doi.org/10.1007/s41208-023-00584-z

51. Kidgell JT, Magnusson M, de Nys R, Glasson CRK (2019) Ulvan: A systematic review of extraction, composition and function. Algal Res 39:101422. https://doi.org/10.1016/j.algal.2019.101422

52. Tsubaki S, Oono K, Hiraoka M, et al (2016) Microwave-assisted hydrothermal extraction of sulfated polysaccharides from Ulva spp. and Monostroma latissimum. Food Chem 210:311–316. https://doi.org/10.1016/j.foodchem.2016.04.121

53. Chen C-Y, Wang S-H, Huang C-Y, et al (2021) Effect of molecular mass and sulfate content of fucoidan from Sargassum siliquosum on antioxidant, anti-lipogenesis, and

anti-inflammatory activity. J Biosci Bioeng 132:359–364. https://doi.org/10.1016/j.jbiosc.2021.06.005

54. Kostas ET, Adams JMM, Ruiz HA, et al (2021) Macroalgal biorefinery concepts for the circular bioeconomy: A review on biotechnological developments and future perspectives. Renew Sustain Energy Rev 151:111553. https://doi.org/10.1016/j.rser.2021.111553

55. Smii H, Leite C, Pinto J, et al (2023) The environmental remediation capacity of Ulva lactuca: the potential of macroalgae to reduce the threats caused by Titanium in marine invertebrate species. Sci Total Environ 858:159586. https://doi.org/10.1016/j.scitotenv.2022.159586

56. Wahlström N, Nylander F, Malmhäll-Bah E, et al (2020) Composition and structure of cell wall ulvans recovered from Ulva spp. along the Swedish west coast. Carbohydr Polym 233:115852. https://doi.org/10.1016/j.carbpol.2020.115852

57. Lahaye M, Robic A (2007) Structure and Functional Properties of Ulvan, a Polysaccharide from Green Seaweeds. Biomacromolecules 8:1765–1774. https://doi.org/10.1021/bm061185q

58. Chappell HF, Jugdaohsingh R, Powell JJ (2020) Physiological silicon incorporation into bone mineral requires orthosilicic acid metabolism to SiO44-. J R Soc Interface 17:20200145. https://doi.org/10.1098/rsif.2020.0145

59. Su Y, Cappock M, Dobres S, et al (2023) Supplemental mineral ions for bone regeneration and osteoporosis treatment. Eng Regen 4:170–182. https://doi.org/10.1016/j.engreg.2023.02.003

60. Tsubaki S, Hiraoka M, Hadano S, et al (2014) Functional group dependent dielectric properties of sulfated hydrocolloids extracted from green macroalgal biomass. Carbohydr Polym 107:192–197. https://doi.org/10.1016/j.carbpol.2014.03.002

61. Matos GS, Pereira SG, Genisheva ZA, et al (2021) Advances in extraction methods to recover added-value compounds from seaweeds: Sustainability and functionality. Foods 10:516. https://doi.org/10.3390/foods10030516

62. Sulastri E, Zubair MS, Lesmana R, et al (2021) Development and characterization of ulvan polysaccharides-based hydrogel films for potential wound dressing applications. Drug Des Devel Ther 15:4213–4226. https://doi.org/10.2147/DDDT.S331120

63. Garcia-Vaquero M, Ummat V, Tiwari B, Rajauria G (2020) Exploring ultrasound, microwave and ultrasound-microwave assisted extraction technologies to increase the extraction of bioactive compounds and antioxidants from brown macroalgae. Mar Drugs 18:172. https://doi.org/10.3390/md18030172

64. Magnusson M, Carl C, Mata L, et al (2016) Seaweed salt from Ulva: A novel first step in a cascading biorefinery model. Algal Res 16:308–316. https://doi.org/10.1016/j.algal.2016.03.018

65. Mukhoro OC, Roos WD, Jaffer M, et al (2018) Very Green Photosynthesis of Gold Nanoparticles by a Living Aquatic Plant: Photoreduction of AuIII by the Seaweed Ulva armoricana. Chem - A Eur J 24:1657–1666. https://doi.org/10.1002/chem.201704448

66. Maldonado-Muñiz M, Luna C, Mendoza-Reséndez R, et al (2020) Silver nanoparticles

against acute hepatopancreatic necrosis disease (AHPND) in shrimp and their depuration kinetics. J Appl Phycol 32:2431–2445. https://doi.org/10.1007/s10811-019-01948-w

67. Gruskiene R, Kavleiskaja T, Staneviciene R, et al (2021) Nisin-Loaded Ulvan Particles: Preparation and Characterization. Foods 10:1007. https://doi.org/10.3390/foods10051007

68. Morelli A, Chiellini F (2010) Ulvan as a new type of biomaterial from renewable resources: Functionalization and hydrogel preparation. Macromol Chem Phys 211:821–832. https://doi.org/10.1002/macp.200900562

69. Madany MA, Abdel-Kareem MS, Al-Oufy AK, et al (2021) The biopolymer ulvan from Ulva fasciata: Extraction towards nanofibers fabrication. Int J Biol Macromol 177:401–412. https://doi.org/10.1016/j.ijbiomac.2021.02.047

70. Consumi M, Leone G, Pepi S, et al (2022) Calcium ions hyaluronan/gellan gum protective shell for delivery of oleuropein in the knee. Int J Polym Mater Polym Biomater 71:414–424. https://doi.org/10.1080/00914037.2020.1848831

71. Kaur K, Kaur G (2013) Formulation and evaluation of chitosan-chondroitin sulphate based nasal inserts for zolmitriptan. Biomed Res Int 2013:958465. https://doi.org/10.1155/2013/958465

72. Pielichowski K, Flejtuch K (2002) Differential scanning calorimetry studies on poly(ethylene glycol) with different molecular weights for thermal energy storage materials. Polym Adv Technol 13:690–696. https://doi.org/10.1002/pat.276

73. Eceiza A, Martin MD, de la Caba K, et al (2008) Thermoplastic Polyurethane Elastomers Based on Polycarbonate Diols With Different Soft Segment Molecular Weight and Chemical Structure: Mechanical and Thermal Properties. Polym Eng Sci 48:297–306. https://doi.org/10.1002/pen.20905

74. Souza HKS, Hilliou L, Bastos M, Gonçalves MP (2011) Effect of molecular weight and chemical structure on thermal and rheological properties of gelling κ/ι-hybrid carrageenan solutions. Carbohydr Polym 85:429–438. https://doi.org/10.1016/j.carbpol.2011.03.006

75. Ma G, Liu Y, Fang D, et al (2012) Hyaluronic acid/chitosan polyelectrolyte complexes nanofibers prepared by electrospinning. Mater Lett 74:78–80. https://doi.org/10.1016/j.matlet.2012.01.012

76. Gajaria TK, Suthar P, Baghel RS, et al (2017) Integration of protein extraction with a stream of byproducts from marine macroalgae: a model forms the basis for marine bioeconomy. Bioresour Technol 243:867–873. https://doi.org/10.1016/j.biortech.2017.06.149

77. Rahimi F, Tabarsa M, Rezaei M (2016) Ulvan from green algae Ulva intestinalis: optimization of ultrasound-assisted extraction and antioxidant activity. J Appl Phycol 28:2979–2990. https://doi.org/10.1007/s10811-016-0824-5

78. Amrutkar JR, Gattani SG (2009) Chitosan-chondroitin sulfate based matrix tablets for colon specific delivery of indomethacin. AAPS PharmSciTech 10:670–677. https://doi.org/10.1208/s12249-009-9253-y

79. Yahyaei B, Peyvandi N, Akbari H, et al (2016) Production, assessment, and

impregnation of hyaluronic acid with silver nanoparticles that were produced by Streptococcus pyogenes for tissue engineering applications. Appl Biol Chem 59:227–237. https://doi.org/10.1007/s13765-016-0147-x

80. Sadhasivam G, Muthuvel A, Pachaiyappan A, Thangavel B (2013) Isolation and characterization of hyaluronic acid from the liver of marine stingray Aetobatus narinari. Int J Biol Macromol 54:84–89. https://doi.org/10.1016/j.ijbiomac.2012.11.028

81. Ghaeini-Hesaroeiye S, Boddohi S, Vasheghani-Farahani E (2020) Dual responsive chondroitin sulfate based nanogel for antimicrobial peptide delivery. Int J Biol Macromol 143:297–304. https://doi.org/10.1016/j.ijbiomac.2019.12.026

82. Gao X, Qu H, Shan S, et al (2020) A novel polysaccharide isolated from Ulva Pertusa: Structure and physicochemical property. Carbohydr Polym 233:115849. https://doi.org/10.1016/j.carbpol.2020.115849

83. Snetkov P, Zakharova K, Morozkina S, Olekhnovich R (2020) Hyaluronic Acid : The Influence of Molecular Weight and Degradable Properties of Biopolymer. Polymers (Basel) 12:1800. https://doi.org/10.3390/polym12081800

84. Beaumont M, Tran R, Vera G, et al (2021) Hydrogel-Forming Algae Polysaccharides: From Seaweed to Biomedical Applications. Biomacromolecules 22:1027−1052. https://doi.org/10.1021/acs.biomac.0c01406

85. Tziveleka LA, Pippa N, Ioannou E, et al (2022) Development of Ulvan-Containing Liposomes as Antibacterial Drug Delivery Platforms. J Funct Biomater 13:186. https://doi.org/10.3390/jfb13040186

86. Espinosa-Antón AA, Zamora-Natera JF, Zarazúa-Villaseñor P, et al (2023) Application of Seaweed Generates Changes in the Substrate and Stimulates the Growth of Tomato Plants. Plants 12:1520. https://doi.org/10.3390/plants12071520

Supplementary Files

This is a list of supplementary files associated with this preprint. Click to download.

- GraphicalAbstract.tiff
- SupplementaryS1.tiff
- SupplementaryS2.tiff